

## A MATHEMATICAL MODEL FOR GAS EXCHANGE IN THE FISH GILL BASED ON NON-LINEAR BLOOD GAS EQUILIBRIUM CURVES

HANS MALTE and ROY E. WEBER

*Institute of Biology, University of Odense, DK-5230 Odense M, Denmark*

**Abstract.** A mathematical model for gas exchange in fish gills is presented, which makes allowance for the non-linear nature of the oxygen and carbon dioxide equilibrium curves of blood, for the uneven distribution of diffusion conductance along the secondary lamellae, and for coupling of oxygen and carbon dioxide exchange through the Bohr and Haldane effects. The model demonstrates that for oxygen loading in the gill the sigmoid equilibrium curve is superior to a linear one, whereas the non-linearity of the carbon dioxide equilibrium curve does not significantly affect carbon dioxide exchange and that the Bohr and Haldane effects have importance only for carbon dioxide exchange. It is also shown that the arterial and expired gas tensions and concentrations are unaffected by whether the bulk of the diffusion conductance is at either the afferent or the efferent end of the individual lamellae, provided that the total conductance is unchanged.

Counter-current flow	Fish gills	Mathematical model
Equilibrium curves	Gas exchange	Ventilation-perfusion ratio

A mathematical model describing gas exchange in fish gills has been put forward by Piiper and Scheid (1972, 1975) and Scheid and Piiper (1976). In this model oxygen and carbon dioxide equilibrium curves are represented by straight lines, and it is assumed that secondary lamellar area, and thereby diffusion conductance, is distributed evenly along the secondary lamellae. These assumptions make it possible to solve the differential equations governing gas exchange analytically. These differential equations and their solutions are exactly equivalent to the ones governing counter-current heat exchange (Holman, 1981). However, as was pointed out by Piiper and Scheid (1975), the above assumptions are incorrect. The aim of the present theoretical study was to develop a model which makes allowance for the non-linearity of the O<sub>2</sub> and CO<sub>2</sub> equilibrium curves of blood, and takes into account the fact, that the equilibrium curves are not 'static' during gas exchange but change with pH and oxygen saturation due to Bohr and Haldane effects. Also, in this study allowance is made for an uneven

*Accepted for publication 8 August 1985*

distribution of secondary lamellar area. This will allow for an assesment of how non-linearity of the content–pressure curves influence arterial contents and pressures compared to the linear models, how the Bohr and Haldane effects influence gas exchange in the gills and how secondary lamellar shape influences gas exchange.

### Development of the model

#### *Symbols used*

$\varphi$ = Bohr effect	$n$ = Hills' coefficient
Ha = Haldane effect	$S$ = oxygen saturation
$P$ = partial pressure	$b$ = slope of the $\text{pH}-\log P_{\text{CO}_2}$ line for blood
$\dot{V}$ = volume flow	$t$ = thickness of membrane separating water and blood
$C$ = concentration	$l$ = length
$h$ = height of secondary lamellae	$L$ = fractional length
$G$ = diffusion conductance	$\beta$ = capacitance coefficient
$\alpha$ = Bunsen coefficient	
$j$ = flux rate	
$k$ = mass transfer coefficient	

#### *Indices*

$i$ = inspired	$w$ = water	$E$ = expired
$\bar{v}$ = mixed venous	$m$ = membrane	$\text{Hb}$ = hemoglobin
$b$ = blood		

#### *Assumptions*

- (1) The mass transfer coefficient of the interlamellar water is independent of  $\dot{V}_w$ .
- (2) The system is in steady state, implying constancy in time of all variables.
- (3) All chemical reactions are in equilibrium.
- (4) There is no diffusion limitation in the blood.
- (5) The system is homogeneous, *i.e.*, all secondary lamellae are perfused and ventilated at the same rate.

#### *Derivations*

In the model the gill is viewed as shown in fig. 1. Water and blood are flowing in counter-current fashion separated by a diffusion barrier. Flow velocities are  $\dot{V}_w$  and  $\dot{V}_b$ . Blood enters at  $l = 0$  with gas tensions  $P\bar{v}_{\text{CO}_2}$ ,  $P\bar{v}_{\text{O}_2}$  and  $\text{pH} = \text{pH}\bar{v}$ , and water enters at  $l = l_0$  with tension  $P_{I\text{O}_2}$  and  $P_{I\text{CO}_2}$ . A steady-state mass balance of oxygen on an element of length  $dl$  and height  $h(l)$  gives

$$\begin{array}{l} \text{blood: } j_2 - j_1 = j_5 \\ \text{water: } j_3 - j_4 = j_5, \quad \text{or} \end{array}$$

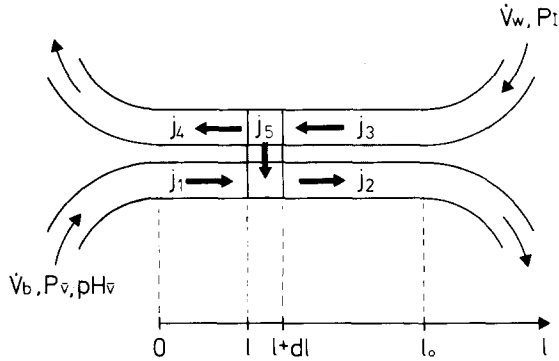


Fig. 1. Schematic view of the gill. Thick arrows indicate transport of oxygen, thin arrows indicate blood and water flow.

$$\text{blood: } \dot{V}b(Cb_{O_2}(l + dl) - Cb_{O_2}(l)) = K_{O_2}h(l)dl(Pw_{O_2}(l) - Pb_{O_2}(l)) \tag{1a}$$

$$\text{water: } \dot{V}w(Cw_{O_2}(l + dl) - Cw_{O_2}(l)) = K_{O_2}h(l)dl(Pw_{O_2}(l) - Pb_{O_2}(l)) \tag{1b}$$

where  $K_{O_2}$  is a compound transfer constant (dimension:  $\text{mM} \cdot \text{min}^{-1} \text{cm}^{-2} \cdot \text{mm Hg}^{-1}$ ) governing the mass transfer in the boundary layer of the interlamellar water as well as the diffusion through the membrane, and is given by (Hills and Hughes, 1970):

$$K_{O_2} = (1/\alpha w_{O_2}k + t/\beta m_{O_2}D_{O_2})^{-1} \tag{1c}$$

where  $k$  is the mass transfer coefficient in water; a quantity that can be evaluated from empirical hydrodynamic flow equations (Holman, 1981; Hills and Hughes, 1970). The accurate value of  $k$  is dependent on  $\dot{V}w$ , but this dependence will be neglected in the following. By making use of the Taylor formula, eqs. 1a and 1b can be written as:

$$\dot{V}b(dCb_{O_2}/dl)dl = K_{O_2}h(l)dl(Pw_{O_2}(l) - Pb_{O_2}(l)) \tag{2a}$$

$$\dot{V}w(dCw_{O_2}/dl)dl = K_{O_2}h(l)dl(Pw_{O_2}(l) - Pb_{O_2}(l)) \tag{2b}$$

For water the relationship between concentration and partial pressure is given by Henry's law, *i.e.*,  $Cw = \alpha wPw$  and 2b thus becomes:

$$dPw_{O_2}/dl = (K_{O_2}h(l)/\dot{V}w\alpha w_{O_2})(Pw_{O_2}(l) - Pb_{O_2}(l)) \tag{3}$$

For blood  $Cb$  will be a function of  $Pb(1)$  and of one or more constants whose value may or may not depend on  $l$ . Thus:

$$Cb_{O_2} = Cb_{O_2}(Pb_{O_2}(l), f_1(l) \dots \dots \dots f_n(l))$$

or

$$Cb_{O_2} = Cb_{O_2}(\dot{f}(l))$$

where  $\vec{r}(l)$  is a vector valued function of  $l$ . Making use of the chain rule for differentiation we can evaluate  $dC_{b_{O_2}}/dl$ :

$$dC_{b_{O_2}}/dl = \nabla C_{b_{O_2}}(\vec{r}) \cdot \vec{r}'(l)$$

where  $\cdot$  means dot product. We now have to choose the function  $C_b$ . We have chosen Hills' equation to describe the oxygen equilibrium curve of fish blood for the following reasons:

- (1) it describes  $C_{b_{O_2}}$  as a function of  $P_{b_{O_2}}$  and contains only two constants namely  $P_{50}$  and  $n$ ,
- (2) these two constants can easily be determined experimentally and are widely used in the literature to describe the oxygen binding properties of fish blood,
- (3) the accuracy gained by using a more elaborate description of the oxygen equilibrium curve such as the Monod, Wyman and Changeux two-state description, or the Adair equation, is minimal compared to the error resulting from the assumptions previously stated.

The relation between concentration and partial pressure is thus:

$$C_{b_{O_2}} = \alpha b_{O_2} P_{b_{O_2}} + 4C_{Hb}(P_{b_{O_2}}^n / (P_{50}^n + P_{b_{O_2}}^n)) \tag{5}$$

Because  $pH$  will vary along the secondary lamella,  $P_{50}$  is a function of  $l$  so that  $C_{b_{O_2}} = C_{b_{O_2}}(P_{50}(l), P_{b_{O_2}}(l))$ .

Thus, from eq. 4:

$$dC_{b_{O_2}}/dl = (\partial C_{b_{O_2}} / \partial P_{b_{O_2}}) (dP_{b_{O_2}}/dl) + (\partial C_{b_{O_2}} / \partial P_{50}) (dP_{50}/dl) \tag{6}$$

inserting this into eq. 2a and solving for  $dP_{b_{O_2}}/dl$  gives the following differential equation

$$dP_{b_{O_2}}/dl = (\partial C_{b_{O_2}} / \partial P_{b_{O_2}})^{-1} [(K_{O_2} h(l) / \dot{V}b) (P_{w_{O_2}}(l) - P_{b_{O_2}}(l)) - (\partial C_{b_{O_2}} / \partial P_{50}) (dP_{50}/dl)] \tag{7}$$

In the  $pH$  range of 7.5–8.0, one can approximate the dependence of  $\log P_{50}$  on  $pH$  by a straight line so that the Bohr effect is given by  $\varphi = \Delta \log P_{50} / \Delta pH$ , which can be reformulated as:

$$P_{50}(l) = P_{50\bar{v}} 10^{\varphi(pH(l) - pH\bar{v})} \tag{8}$$

By differentiation of  $P_{50}$  with respect to  $l$  and inserting this into eq. 7 and simultaneously making the substitutions  $L = l/l_0$  and  $Gd_{O_2}(L) = K_{O_2} h(L)l_0$  in eqs. 3 and 7 we finally get:

$$dP_{b_{O_2}}/dL = (\partial C_{b_{O_2}} / \partial P_{b_{O_2}})^{-1} [(Gd_{O_2}(L) / \dot{V}b) (P_{w_{O_2}}(L) - P_{b_{O_2}}(L)) - 2.303 P_{50}(L) \varphi (\partial C_{b_{O_2}} / \partial P_{50}) (dpH/dL)] \tag{9a}$$

$$dP_{w_{O_2}}/dL = (Gd_{O_2}(L) / \dot{V}w \alpha w) (P_{w_{O_2}}(L) - P_{b_{O_2}}(L)) \tag{9b}$$

An analysis of CO<sub>2</sub> exchange gives two equations analogous to eqs. 2a and 2b:

$$\dot{V}b(dCb_{CO_2}/dl)dl = K_{CO_2}h(l)dl(Pb_{CO_2}(l) - Pw_{CO_2}(l)) \quad (10a)$$

$$\dot{V}w(dCw_{CO_2}/dl)dl = K_{CO_2}h(l)dl(Pb_{CO_2}(l) - Pw_{CO_2}(l)) \quad (10b)$$

There is a fixed relation between K<sub>CO<sub>2</sub></sub> and K<sub>O<sub>2</sub></sub>, *i.e.*, K<sub>CO<sub>2</sub></sub> = AK<sub>O<sub>2</sub></sub> where A is a constant. As can be seen from eq. 1c, the value of A depends on the values of k and D/t. If k is large compared to D/t, the relation will be approximated by (Randall, 1970):

$$K_{CO_2}/K_{O_2} \approx \beta m_{CO_2} D_{CO_2} / \beta m_{O_2} D_{O_2} = 37 \text{ at } 10^\circ \text{C}$$

When D/t is large compared to k it will be approximated by (Randall, 1970):

$$K_{CO_2}/K_{O_2} \approx \alpha w_{CO_2} / \alpha w_{O_2} = 31 \text{ at } 10^\circ \text{C}$$

Hills and Hughes (1970) in a dimensional analysis of fish gills concluded that 80–90% of the diffusion resistance is due to interlamellar water. Scheid and Piiper (1971), using a different type of model arrived at a value of 25%. Considering the widely different estimates, and recognizing that this proportion will vary with ventilation, we chose the mean of the extremes; A = 34. To find function Cb<sub>CO<sub>2</sub></sub>(Pb<sub>CO<sub>2</sub></sub>(l), f<sub>1</sub>(l), ..., f<sub>n</sub>(l)) we rearrange the equation describing the dependence of pH on total CO<sub>2</sub> concentration and pK' (Albers, 1970):

$$Cb_{CO_2} = \alpha b_{CO_2} Pb_{CO_2} (1 + 10^{(pH - pK')}) \quad (11)$$

pK' is dependent on pH and temperature as documented by Severinghaus (1971). These data fit the following equation at 10 °C:

$$pK' = pK^\circ - (pH - pH^\circ)0.09 \quad (12)$$

where pK<sup>°</sup> = 6.194 and pH<sup>°</sup> = 7.6. pH can be expressed as a linear function of logP<sub>CO<sub>2</sub></sub>, as is done in the well known logP<sub>CO<sub>2</sub></sub> vs pH diagram (Siggaard-Andersen, 1974; Albers, 1970):

$$pH = pH\bar{v} + b \log(Pb_{CO_2}/P\bar{v}_{CO_2}) \quad (13)$$

Both the slope and the intercept of this curve are altered by a change in the oxygenation state of hemoglobin due to the Haldane effect. Neglecting the change in slope, which is of minor importance, and assuming that the Haldane effect is independent of hemoglobin saturation, eq. 13 can be written:

$$pH = pH\bar{v} - Ha(S - S\bar{v}) + b \log(Pb_{CO_2}/P\bar{v}_{CO_2}) \quad (14)$$

Insertion of eqs. 12 and 14 into eq. 11 and rearranging gives:

$$Cb_{CO_2} = \alpha b_{CO_2} Pb_{CO_2} + \alpha b_{CO_2} B Pb_{CO_2}^{(1.09b + 1)} \quad (15)$$

where

$$B = P\bar{v}_{CO_2}^{-1.09b} 10^{(1.09(pH\bar{v} - Ha(S - S\bar{v})) - pK^{\circ} - 0.09pH^{\circ})} \quad (16)$$

Recognizing that  $Cb_{CO_2} = Cb_{CO_2}(Pb_{CO_2}(l), S(l))$  and proceeding in the same manner as was done for oxygen, we finally arrive at two differential equations describing  $CO_2$  exchange:

$$dPw_{CO_2}/dL = -(AGd_{O_2}(L)/\dot{V}_w \alpha w_{CO_2})(Pb_{CO_2}(L) - Pw_{CO_2}(L)) \quad (17a)$$

$$dPb_{CO_2}/dL = -(\partial Cb_{CO_2}/\partial Pb_{CO_2})^{-1} [(AGd_{O_2}(L)/\dot{V}_b)(Pb_{CO_2}(L) - Pw_{CO_2}(L)) + (\partial Cb_{CO_2}/\partial S)(dS/dL)] \quad (17b)$$

As in the case of eqs. 9a and b, eqs. 17a and b constitute a system of two first-order differential equations with the unknowns  $Pb$  and  $Pw$ . These two systems are linked through the Bohr and Haldane effects. With the help of eq. 14 they can be solved numerically by a fourth-order Runge-Kutta iteration. The solution gives the oxygen and carbon dioxide tensions in water and blood as well as the pH as functions of  $L$ . As byproducts we also get the hemoglobin saturation and the oxygen and carbon dioxide concentrations as functions of  $L$ . Once these profiles are known the following quantities can be calculated:

$\dot{M}$  = gas exchange rate

$E_b$  = blood effectivity =  $\dot{M}(\text{actual})/\dot{M}(Pa = Pi)$

$E_w$  = water effectivity =  $\dot{M}(\text{actual})/\dot{M}(PE = P\bar{v})$

$E_t$  = transfer effectivity =  $1 - E_b - E_w$

$Li_v$  = ventilation limitation =  $1 - \dot{M}(\text{act.})/\dot{M}(Vw = \infty)$

$Li_p$  = perfusion limitation =  $1 - \dot{M}(\text{act.})/\dot{M}(vb = \infty)$

$Li_D$  = diffusion limitation =  $1 - \dot{M}(\text{act.})/\dot{M}(Gd = \infty)$

The differential equations were subjected to the following initial and boundary values chosen to fit rainbow trout at  $10^{\circ}C$ : Initial values:  $Pb_{O_2}(0) = P\bar{v}_{O_2} = 25$  mm Hg,  $Pb_{CO_2}(0) = P\bar{v}_{CO_2} = 3.5$  mm Hg,  $pH(0) = pH\bar{v} = 7.70$

Boundary values:  $Pw_{O_2}(1) = PI_{O_2} = 150$  mm Hg,  $Pw_{CO_2}(1) = PI_{CO_2} = 0.3$  mm Hg

The following constants were chosen to fit rainbow trout at  $10^{\circ}C$ :  $C_{Hb} = 0.93$  mM  $L^{-1}$ ,  $P_{50\bar{v}} = 22$  mm Hg,  $\varphi = -0.50$ ,  $Ha = 0.05$ ,  $b = -0.70$ . The Bunsen coefficients used are those given by Boutilier *et al.* (1984). Unless otherwise stated,  $Gd$  was evenly distributed *i.e.*  $Gd(L) = Gd$ .

**Results**

Figure 2 shows the arterial gas tensions and concentrations as a function of  $\dot{V}_w/\dot{V}_b$  and  $G_d/\dot{V}_b$ . In a model such as that of Piiper and Scheid's (1975) where linear gas equilibrium curves are assumed it is common to present various data as functions of the capacity-rate ratio ( $\dot{V}_w\beta_w/\dot{V}_b\beta_b$ ) and the number of transfer units ( $G_d/\dot{V}_b\beta_b$ ). This is, however, not possible in this model because  $\beta_b$  now varies as gas exchange proceeds.

For the oxygen tension curve one can clearly distinguish 3 regimes of  $\dot{V}_w/\dot{V}_b$ . At low  $\dot{V}_w/\dot{V}_b$  ( $< 3$ ) gas exchange show slight dependence on  $\dot{V}_w/\dot{V}_b$  and the dependence on  $G_d/\dot{V}_b$  is practically nil. At  $\dot{V}_w/\dot{V}_b$  between 3 and 20 there is strong dependence on  $\dot{V}_w/\dot{V}_b$  and  $G_d/\dot{V}_b$  and at  $\dot{V}_w/\dot{V}_b > 20$  there is strong dependence only on  $G_d/\dot{V}_b$ , especially at  $G_d/\dot{V}_b < 23$ . For the oxygen concentration curve the dependence on  $\dot{V}_w/\dot{V}_b$  begins much earlier indicating that oxygen tension is held down while oxygen is loaded in the gills and rises only towards the end of loading.

The carbon dioxide concentration and tension curves resemble each other much more than was the case for oxygen, reflecting the fact that the carbon dioxide equilibrium curve is much closer to being a straight line than the oxygen equilibrium curve. Figure 2

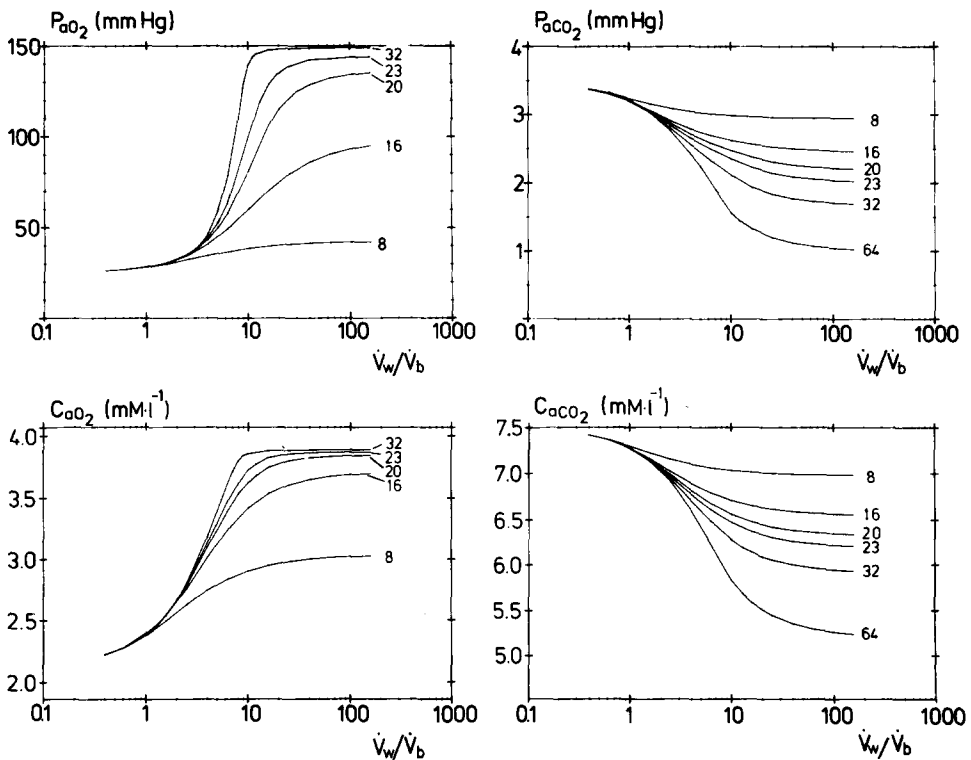


Fig. 2. Oxygen and carbon dioxide tensions and concentrations in arterial blood as a function of  $\dot{V}_w/\dot{V}_b$  at different  $G_d/\dot{V}_b$  values, the latter in  $\mu\text{M L}^{-1} \text{mm Hg}^{-1}$ .

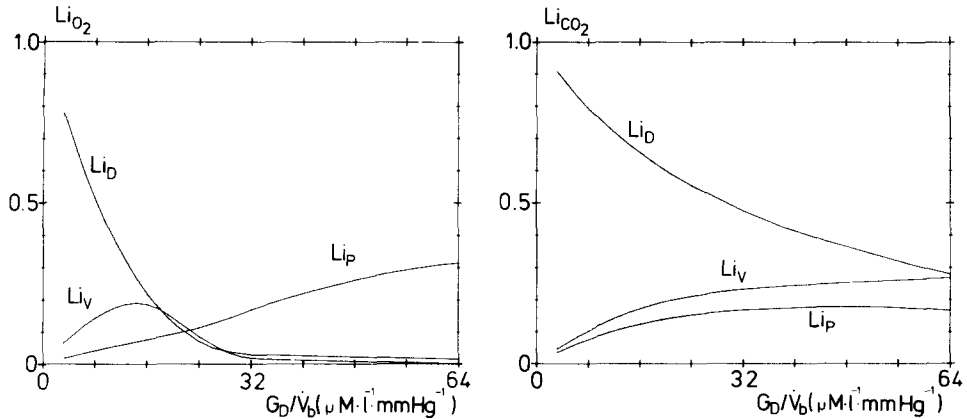


Fig. 3. Limitations of gas exchange. A, oxygen; B, carbon dioxide.

clearly demonstrates two very powerful means of regulating oxygen loading and carbon dioxide unloading in the gills.

Figure 3 shows the limitations as a function of  $G_D/\dot{V}_b$  at a  $\dot{V}_w/\dot{V}_b$  of 10. Here the difference between the oxygen and carbon dioxide exchange is very clear. Whereas carbon dioxide is dominated by diffusion limitation throughout the range of  $G_D/\dot{V}_b$  values tested, oxygen is dominated by diffusion limitation only at  $G_D/\dot{V}_b$  values less than 19 and by perfusion limitation at higher  $G_D/\dot{V}_b$  values.

To trace whether the non-linearity of the oxygen and carbon dioxide equilibrium curves has any effect on the arterial tensions and concentrations, a comparison was made with Piiper and Scheid's model. To do this a run of the present model was made establishing the functional equilibrium curve followed during loading/unloading for each  $\dot{V}_w/\dot{V}_b$  (in fact only venous and arterial points were used) and the slope of the straight line connecting the arterial and venous points was computed ( $=\beta b$ ). Now the capacity-rate ratio could be calculated from  $CRR = (\dot{V}_w/\dot{V}_b) \cdot (\beta w/\beta b)$  and the number of transfer units from  $NTU = (G_D/\dot{V}_b) \cdot (1/\beta b)$ , thus making it possible to compute the tensions and concentrations from the exponential expressions of Piiper and Scheid (1975). Figure 4 shows a comparison of concentrations and tensions between the two models. It shows very clearly that at  $\dot{V}_w/\dot{V}_b > 8$  considerably greater arterial oxygen concentrations are attained with the non-linear equilibrium curve, and furthermore this is at a considerably higher tension (*i.e.*, potential) which is of importance to unloading in the tissues. Figure 4 also demonstrates that for  $CO_2$  the difference between the two models is negligible. Further illustrating the difference between the two models with regard to oxygen loading, fig. 5 shows the water and blood tension profiles together with the blood concentration profiles along the secondary lamella for one particular set of  $\dot{V}_w/\dot{V}_b$ ,  $G_D/\dot{V}_b$  values. As evident blood  $O_2$  tension is initially kept lower in the present model thereby keeping the gradient greater and permitting greater entry of oxygen. Only towards the end of the lamella the oxygen tension rises and exceeds that predicted by the Piiper/Scheid model. It is noteworthy that neither of the profiles are linear; that in

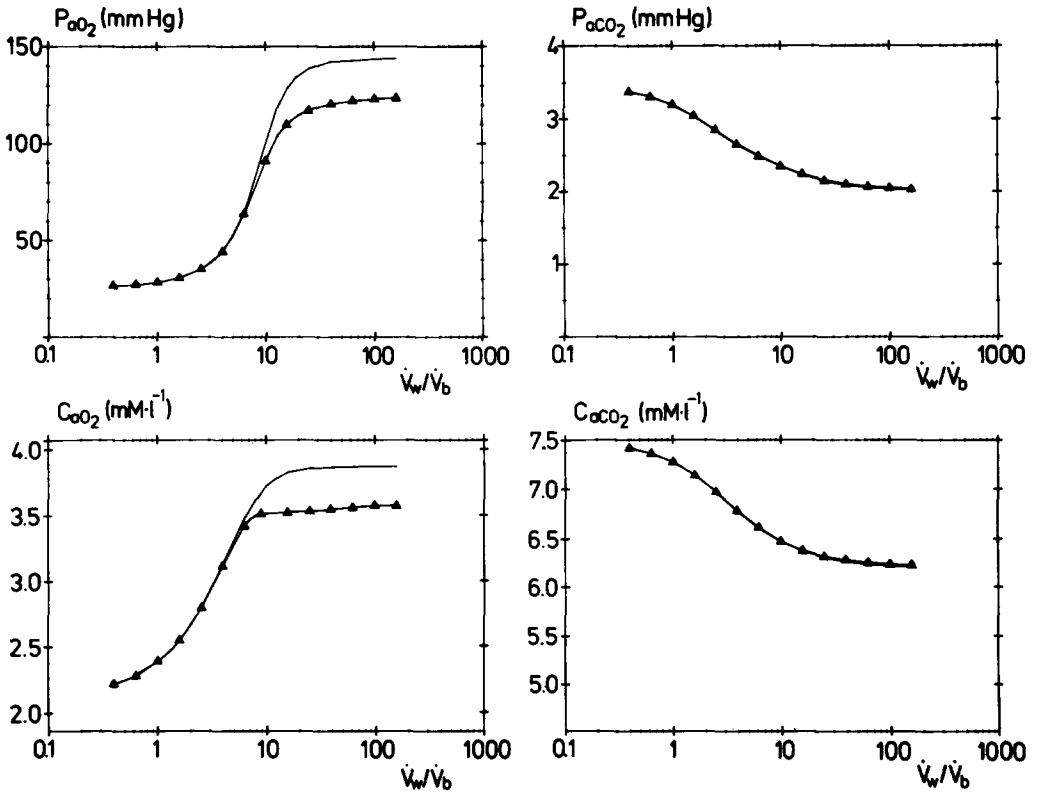


Fig. 4. Comparison of two models of gas exchange. The figure shows oxygen and carbon dioxide tensions and concentrations as a function of  $\dot{V}_w/\dot{V}_b$  at  $G_d/\dot{V}_b = 23 \mu M L^{-1} mm Hg^{-1}$ . Triangles represent the straight equilibrium curve model, curves without symbols represent the present model.

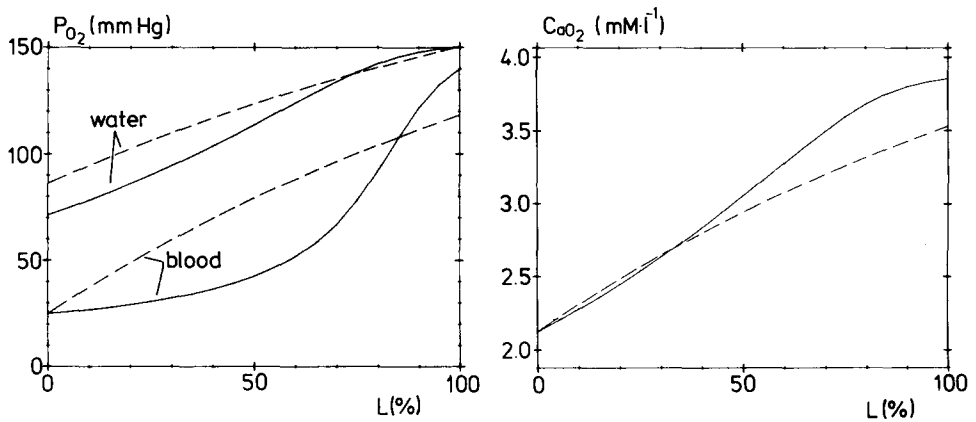


Fig. 5. Oxygen tensions in water and blood and oxygen concentration in blood as a function of fractional length (L) in two models of gas exchange. Drawn lines represent the present model, broken lines represent the straight equilibrium curve model. A, tensions; B, concentrations.

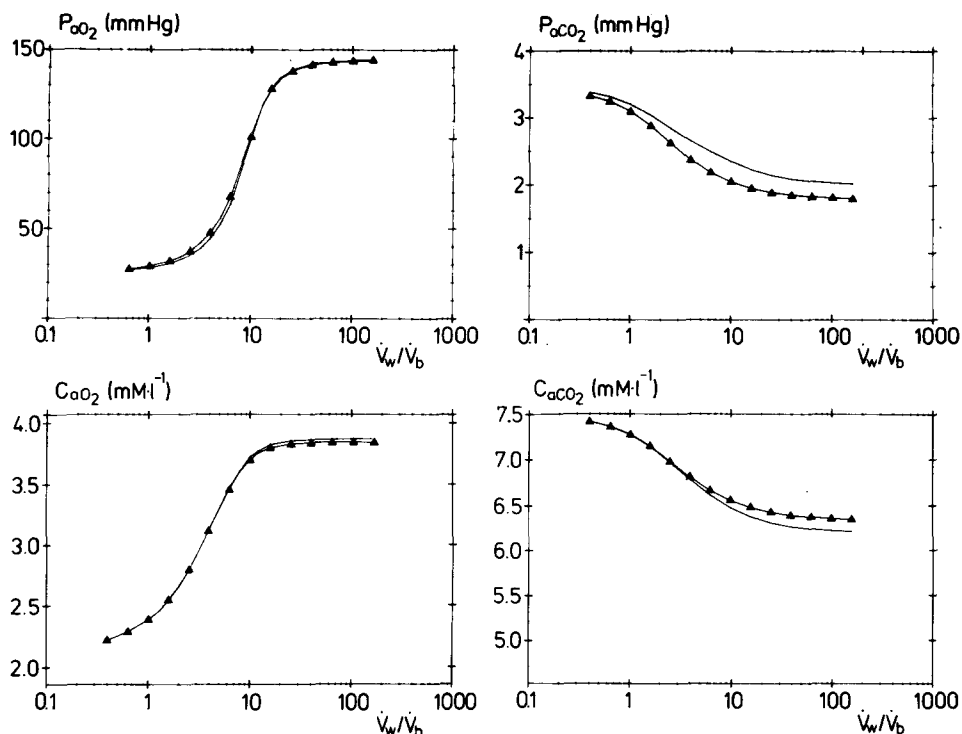


Fig. 6. Effect of the Bohr and Haldane effects on gas exchange. The figure shows oxygen and carbon dioxide tensions and concentrations as a function of  $\dot{V}_w/\dot{V}_b$  at  $G_d/\dot{V}_b = 23 \mu\text{M L}^{-1} \text{mm Hg}^{-1}$ . Triangles represent absence of Bohr and Haldane effects, curves without symbols represent the presence of Bohr and Haldane effects.

the present model being sigmoidal and that of the Piiper/Scheid model being exponential (the latter profiles in fact degenerate into two straight lines in the special case when  $\text{CRR} = 1.0$ , which can be proven by use of L' Hopitals rule on expression 12 in Scheid and Piiper, 1976). Figure 6 shows the effect of removing the Bohr and Haldane effects. As can be seen there is very little effect on oxygen loading although at  $\dot{V}_w/\dot{V}_b > 10$  there is a 2% greater arterial oxygen concentration when the Bohr and Haldane effects are operational. On the contrary, there is a more marked effect on  $\text{CO}_2$  unloading, the arterial  $\text{CO}_2$  concentration being significantly smaller in the presence of the Bohr and Haldane effects. At the same time, however, the  $\text{CO}_2$  is left in the blood at a higher pressure (*i.e.*, potential). Figure 7 shows the effect of distributing the same total secondary lamellar area (and thereby  $G_d$ ) in two different ways on the oxygen tension profiles in water and blood. As can be seen, the profiles are very different but the resulting arterial and expired  $\text{O}_2$  tensions are exactly the same.

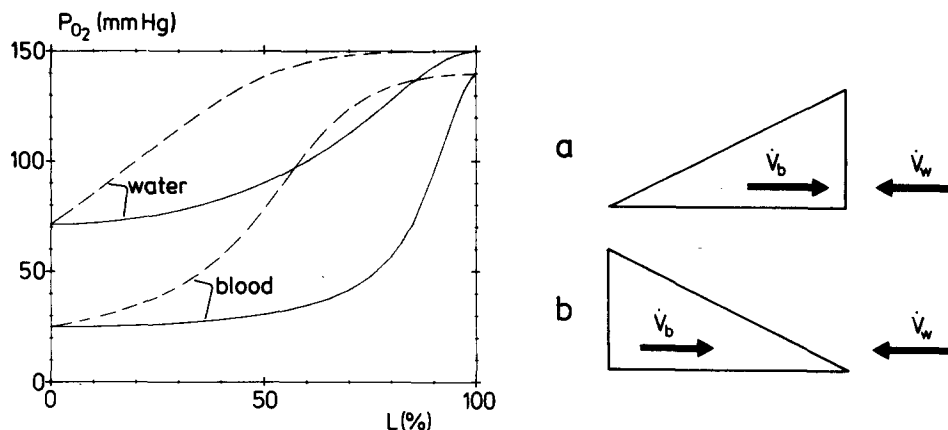


Fig. 7. Effect of distributing the same total secondary lamellar area in two different ways on oxygen tensions in water and blood. Solid line corresponds to a, broken line corresponds to b.

## Discussion

The resting *in vivo* value of arterial  $P_{O_2}$  of rainbow trout is approximately 100 mm Hg (Nikinmaa, 1981; Davis and Cameron, 1971). Assuming a ventilation-perfusion ratio of 10 which is normal in rainbow trout (Davis and Cameron, 1971)  $Gd/\dot{V}_b^*$  will be about 23 as evident from fig. 2. With this combination of  $\dot{V}_w/\dot{V}_b$  and  $Gd/\dot{V}_b$  it can be seen from fig. 3 that uptake of oxygen is mostly perfusion limited although some ventilation and diffusion limitation also is present. This is in agreement with Daxboeck *et al.* (1982) who found that oxygen transfer across the gills of a spontaneously-ventilated, blood-perfused trout preparation was directly proportional to blood flow in the range of 10–25 ml min<sup>-1</sup> kg<sup>-1</sup>. It is, however, obvious from fig. 1 that although this model shows a perfusion limitation, a doubling of blood flow would not lead to a doubling of oxygen uptake as the  $Gd/\dot{V}_b$  would be halved as would  $\dot{V}_w/\dot{V}_b$  thereby reducing the arterial oxygen concentration considerably. Possible explanations for the strong dependence of  $\dot{M}_{O_2}$  on  $\dot{V}_b$  observed by Daxboeck *et al.* (1982) are: (1) the very low hematocrit used in their preparation, (2) that  $Gd$  likely will have risen along with  $\dot{V}_b$ , partly due to distension of the secondary lamellae caused by the elevated blood pressure (Soivio and Tuurala, 1981), and partly due to recruitment of secondary lamellae caused by the elevated pulse pressure (Farrel *et al.*, 1979), and (3) the possibility that the fish itself responded to the elevated blood flow by adjusting ventilation and/or  $Gd$  so as to keep a constant  $Pa_{O_2}$ , particularly since the fish were able to raise their ventilation in response to environmental hypoxia.

Carbon dioxide elimination as indicated by  $Gd/\dot{V}_b = 23$  and  $\dot{V}_w/\dot{V}_b = 10$  is strongly diffusion limited, which is in accordance with Piiper and Scheid's (1975) finding in their

\* Note that  $Gd/\dot{V}_b$  is not a dimensionless ratio but has a dimension like capacitance, for instance  $\mu\text{M L}^{-1} \text{mm Hg}^{-1}$ .

model for the dogfish gill. Cameron and Polhemus (1974) using a completely different kind of model for CO<sub>2</sub> elimination (which takes into account reaction rates of the entire CO<sub>2</sub> system) similarly found that elimination was highly sensitive to the diffusion conditions. It is important to note that even though one of the limitations of gas exchange may dominate (which need not be the case) the two other most likely also may occur. As revealed in fig. 4, it is advantageous for fish to have sigmoid oxygen equilibrium curves. Figure 5 illustrates that the advantage over a linear curve is that it keeps  $P_{bO_2}$  low at the beginning which causes a larger O<sub>2</sub> gradient whereby more oxygen will diffuse inwards. Although this is intuitively logical, this paper provides the first mathematical demonstration of its validity. From fig. 5 it is clear, that by using the common estimate of the mean tension gradient,  $\overline{\Delta P} = 1/2(P_I + P_E) - 1/2(P_a + P_{\bar{v}})$ , one underestimates the true mean gradient, thereby overestimating the diffusion conductance, as calculated from:

$$Gd = \dot{M}_{O_2} / \overline{\Delta P}_{O_2} \quad (18)$$

With  $Gd/\dot{V}_b = 23 \mu\text{M L}^{-1} \text{ mm Hg}^{-1}$ , and assuming a resting  $\dot{V}_b$  of  $18 \text{ ml min}^{-1} \cdot \text{kg}^{-1}$  (Davis and Cameron, 1970), the  $Gd$  will be  $0.414 \mu\text{M min}^{-1} \text{ mm Hg}^{-1} \text{ kg}^{-1}$ . Still using  $\dot{V}_w/\dot{V}_b = 10$ , an  $\dot{M}_{O_2}$  of  $28.7 \mu\text{M min}^{-1} \text{ kg}^{-1}$  is obtained. Calculating  $Gd$  from eq. 18, using the common estimate of the mean gradient, one arrives at  $Gd = 0.567 \mu\text{M min}^{-1} \text{ mm Hg}^{-1} \text{ kg}^{-1}$ , which is an overestimation of 37%. The use of the mean gradient produced by the Piiper-Scheid model, the so-called log-mean gradient (Scheid and Piiper, 1976), also leads to an overestimation of  $Gd$ ; using the same example, the resulting  $Gd$  will be exactly the same, namely  $0.567 \mu\text{M min}^{-1} \text{ mm Hg}^{-1} \text{ kg}^{-1}$ . As an alternative, Piiper and Scheid suggest, that the diffusion conductance is calculated by a modified Bohr-integration technique, which takes into account the non-linear equilibrium curves. Their method, however, divides the secondary lamella into  $n$  pieces, assumed to have equal oxygen uptake ( $= \dot{M}_{O_2}/n$ ), which in general will not be true (for instance this assumption implies linear tension profile in the water). Remembering that in the model presented here, the arterial and expired tensions are dependent variables, *i.e.*,  $P_a = f_1(P_{\bar{v}}, P_I, \dot{V}_b, \dot{V}_w, Gd)$  and  $P_E = f_2(P_{\bar{v}}, P_I, \dot{V}_b, \dot{V}_w, Gd)$ , it is not difficult, when knowing  $P_a, P_I, P_{\bar{v}}, P_E$  and  $\dot{M}_{O_2}$  (thereby also  $\dot{V}_b$  and  $\dot{V}_w$ ), to solve numerically for  $Gd$ , which is now the only unknown. The  $Gd$  value found in this way is independent of the assumption of equally distributed  $\dot{M}_{O_2}$ , and takes into account the non-linear equilibrium curves as well as the Bohr and Haldane effects.

The importance of the link of the O<sub>2</sub> and CO<sub>2</sub> transport through the Bohr and Haldane effects, is illustrated in CO<sub>2</sub> elimination which, as can be seen in fig. 6, is enhanced at higher  $\dot{V}_w/\dot{V}_b$  values ( $> 10$ ). This effect becomes even more marked at higher  $Gd/\dot{V}_b$ , which means that the effect of increasing  $\dot{V}_w/\dot{V}_b$  and  $Gd/\dot{V}_b$  on the CO<sub>2</sub> elimination, becomes greater. For oxygen, on the contrary, there is only a very small effect on the tension and content so that it is not the gills where the Bohr and Haldane effects appear to be of greatest importance in oxygen exchange. Intuitively one might expect that the distribution of the secondary lamellar area, and thereby  $Gd$ , would influence gas exchange. Indeed Hughes (1972), based on a method developed by

Hughes and Hills (1971), calculated the tension profiles along the gill for various shapes of secondary lamellae, and on this basis concluded that it was most effective to place the greater part of the lamellar area at the end where the water enters. In this model the water and blood tensions were fixed at both ends of the lamella, and the profiles connecting arterial and venous points were calculated. This procedure having  $P_a$  and  $P_E$  as independent variables conceals the fact that the only values of importance to the fish are those in blood at the end point, and that it is irrelevant how this was reached. The present model, with  $P_a$  and  $P_E$  being dependent variables, clearly shows that no matter how secondary lamellar area is distributed, arterial and expired points are the same. It follows that no particular shape of secondary lamella is preferable to ensure effective gas exchange. Indirectly, however, lamella shape can of course exert some effect on gas exchange, through its influence on water flow, a factor not dealt with in this paper.

#### *Limitations of the model*

The actual conditions in the gill deviate from the idealized model in a number of ways which could affect the results of the present analysis. Among the most important are:

(1) *Cyclic changes in  $\dot{V}_w$  and  $\dot{V}_b$ .* The steady-state assumption is invalidated by the fact that both ventilation and perfusion are cyclic processes. The incorporation of this in the model leads to 4 partial differential equations instead of ordinary differential equations, the solution of which is extremely complex, and has not yet been performed. Such an analysis has been performed on the non-diffusion limited mammalian lung (Crandall and Flumerfelt, 1967; Lin and Shir, 1974), which mathematically speaking is a simpler system. These analyses show that pulsatile flow has a negative effect on the efficiency of gas exchange, and that this effect increases as pulsatility increases (Lin and Shir, 1974). On the other hand, this effect is partially compensated for if simultaneous fluctuation of capillary bed volume is taken into consideration (Bidani *et al.*, 1978).

(2) *Finite reaction rates.* Reaction rates will not, as assumed in this model, be infinite. Especially carbon dioxide elimination is complex and two possible rate-limiting steps may be the hydration of  $\text{CO}_2$  and the chloride shift. Indeed, Cameron and Polhemus (1974) in their model found  $\text{CO}_2$  elimination to be highly sensitive to the catalysis factor (the red cell/plasma ratio of the  $\text{CO}_2$  hydrolysis rate) and less sensitive to the rate of the chloride shift. There also seems to be experimental evidence for this since Perry *et al.* (1982) found in a spontaneously-ventilated blood-perfused trout preparation that, at the same input concentration of  $\text{CO}_2$ , the elimination was linearly dependent on hematocrit. With an overall association constant of  $1-4 \times 10^7 \text{ L M}^{-1} \text{ S}^{-1}$  (20 °C; Brunori, 1975) it seems unlikely that oxygen uptake should be limited by reaction velocities. This is corroborated by the finding of Hughes and Koyama (1975) and Hills *et al.* (1982), by direct measurement that the deoxygenation and oxygenation reaction velocity of hemoglobin in the intact red cells in secondary lamellae of carp and eel appears to be of little importance compared to the diffusion resistance.

(3) *Uneven distribution of  $\dot{V}_w$  and  $\dot{V}_b$ .* It has been known for decades in human respiratory physiology that ventilation and blood flow is unevenly distributed to the different compartments (*i.e.*, alveoli) of the lung and that this may cause serious impairment of gas exchange. It was first shown by the introduction of the oxygen-carbon dioxide diagram (Riley and Cournand, 1949) and later in computer models of the lung (West, 1969). In addition, it was mathematically proven by Evans *et al.* (1974) that under physiological conditions, this occurs regardless of the shape of the equilibrium curves of blood. There is no reason to believe that fish gills are evenly ventilated and perfused. And there is no doubt that this will have an impairing effect on gas exchange, as seen by lowered  $P_{aO_2}$  and  $Ca_{O_2}$  and heightened  $P_{aCO_2}$  and  $Ca_{CO_2}$ . This has been confirmed by Piiper and Scheid in a two-compartment, non-diffusion-limited, straight equilibrium curve model of the fish gill. Their model study demonstrates that any distribution of  $\dot{V}_w/\dot{V}_b$  that is different from an even distribution will impair gas exchange.

(4) *Shunts.* Any shunting of venous blood away from the respiratory surface and subsequent mixing with blood having a higher oxygenation level will impair gas exchange. There is evidence that in most teleosts there are no arterio-arterial shunts bypassing the secondary lamellae (Vogel, 1978; Laurent and Dunel, 1976). Recent investigations, however, have shown that the basal channels of the secondary lamellae, which are deeply buried in the gill filament, may function as intralamellar blood shunts (Pärt *et al.*, 1984; Tuurala *et al.*, 1984). Also shunting of water, for instance between the tips of the gill filaments is possible, which also will impair gas exchange.

(5) *Gill metabolism.* As oxygen diffuses through the epithelial tissue of the gill the oxygen tension in the epithelial cells must be greater than in the arterial blood. Therefore the epithelial cells must be supplied by oxygen from the water, which will slow the diffusion into the blood. In addition it has been shown that gill tissue metabolism uses oxygen from blood which later appears in the dorsal aorta, thereby lowering  $P_{aO_2}$  and  $Ca_{O_2}$  and raising  $P_{aCO_2}$  and  $Ca_{CO_2}$  (Wood *et al.*, 1978; Daxboeck *et al.*, 1982; Pärt *et al.*, 1984). Estimations from these authors of the magnitude of the gill oxygen consumption range from 8 to 27% of the total resting oxygen consumption.

(6) *Dependence of  $k$  on  $\dot{V}_w$ .* The mass transfer coefficient of the interlamellar water will vary with  $\dot{V}_w$  in a manner depending on the prevalent flow conditions. Based on calculations of the Reynold's number, it is probable that the flow is laminar at all ventilation volumes encountered *in vivo* (Randall and Daxboeck, 1984). This was also the conclusion reached by Hills and Hughes (1970) in a dimensional analysis of gas transfer in fish gills. Under these circumstances the mass transfer coefficient will be given by:

$$k = c \dot{V}_w^{1/3}$$

modified from Holman (1981), where  $c$  is a constant. From the equation it is evident that the mass transfer coefficient is dependent on  $\dot{V}_w$ , which was also pointed out by Scheid and Piiper (1971) in their model study of respiratory gas equilibration in interlamellar water. This relationship is beneficial to the fish, as  $G_d$  thereby will rise in situations where the oxygen transport system is stressed, for instance in exercise and under hypoxia where ventilation is raised.

## References

- Albers, C. (1970). Acid-base balance. In: Fish Physiology. Vol. IV, edited by W. S. Hoar and D. J. Randall. New York, Academic Press, pp. 173–208.
- Bidani, A., R. W. Flumerfelt and E. D. Crandall (1978). Analyses of the effect of pulsatile capillary blood flow and volume on gas exchange. *Respir. Physiol.* 35: 27–42.
- Boutilier, R. G., T. A. Heming and G. K. Iwama (1984). Physicochemical parameters for use in fish respiratory physiology. In: Fish Physiology. Vol. XA, edited by W. S. Hoar and D. J. Randall. New York, Academic Press, pp. 403–430.
- Brunori, M. (1975). Molecular adaptation to physiological requirements: The hemoglobin system of the trout. *Curr. Top. Cell. Regul.* 9: 1–39.
- Cameron, J. N. and J. A. Polhemus (1974). Theory of CO<sub>2</sub> exchange in trout gills. *J. Exp. Biol.* 60: 183–194.
- Crandall, E. D. and R. W. Flumerfelt (1967). Effect of time-varying blood flow on oxygen uptake in the pulmonary capillaries. *J. Appl. Physiol.* 23: 944–953.
- Davis, J. C. and J. N. Cameron (1971). Water flow and gas exchange at the gills of rainbow trout, *Salmo gairdneri*. *J. Exp. Biol.* 54: 1–18.
- Daxboeck, C., P. S. Davie, S. F. Perry and D. J. Randall (1982). The spontaneously ventilating blood perfused trout preparation: Oxygen transfer across the gills. *J. Exp. Biol.* 101: 35–45.
- Evans, J. W., P. D. Wagner and J. B. West (1974). Conditions for reduction of pulmonary gas transfer by ventilation-perfusion inequality. *J. Appl. Physiol.* 36: 533–537.
- Farrell, A. P., C. Daxboeck and D. J. Randall (1979). The effect of input pressure and flow on the pattern and resistance to flow in the isolated perfused gill of a teleost fish. *J. Comp. Physiol.* 133: 233–240.
- Hills, B. A. and G. M. Hughes (1970). A dimensional analysis of oxygen transfer in the fish gill. *Respir. Physiol.* 9: 126–140.
- Hills, B. A., G. M. Hughes and T. Koyama (1982). Oxygenation and deoxygenation kinetics of red cells in isolated lamellae of fish gills. *J. Exp. Biol.* 98: 269–275.
- Holman, J. P. (1981). Heat Transfer. New York, McGraw Hill, 570 p.
- Hughes, G. M. and B. A. Hills (1971). Oxygen tension distribution in water and blood at the secondary lamella of the dogfish gill. *J. Exp. Biol.* 55: 399–408.
- Hughes, G. M. (1972). Distribution of oxygen tension in the blood and water along the secondary lamella of the icefish gill. *J. Exp. Biol.* 56: 481–492.
- Hughes, G. M. and T. Koyama (1975). Gas exchange of single red blood cells within secondary lamellae of fish gills. *J. Physiol. (London)* 246: 82–83.
- Laurent, P. and S. Dunel (1976). Functional organization of the teleost gill. I. Blood pathways. *Acta Zool.* 57: 189–209.
- Lin, K. H. and C. C. Shir (1974). A numerical model of O<sub>2</sub> uptake in the human lung during a respiratory cycle. *Math. Biosci.* 19: 319–342.
- Nikinmaa, N. (1981). Respiratory adjustment of rainbow trout (*Salmo gairdneri*, Richardson) to changes in environmental temperature and oxygen availability. Ph.D. thesis, University of Helsinki.
- Pärt, P., H. Tuurala, M. Nikinmaa and A. Kiessling (1984). Evidence for a non-respiratory intralamellar shunt in perfused rainbow trout gills. *Comp. Biochem. Physiol.* 79: 29–34.
- Perry, S. F., P. S. Davie, C. Daxboeck and D. J. Randall (1982). A comparison of CO<sub>2</sub> excretion in a

- spontaneously ventilating, blood-perfused trout preparation and saline-perfused gill preparations: Contribution of the branchial epithelium and red blood cell. *J. Exp. Biol.* 101: 47–60.
- Piiper, J. and P. Scheid (1972). Maximum gas transfer efficacy of models for fish gills, avian lungs and mammalian lungs. *Respir. Physiol.* 14: 115–124.
- Piiper, J. and P. Scheid (1975). Gas transport efficacy of gills, lungs and skin: Theory and experimental data. *Respir. Physiol.* 23: 209–221.
- Piiper, J. and P. Scheid (1984). Model analysis of gas transfer in fish gills. In: *Fish Physiology*. Vol. XA, edited by W. S. Hoar and D. J. Randall. New York, Academic Press, pp. 229–262.
- Randall, D. J. (1970). Gas exchange in fish. In: *Fish Physiology*. Vol. IV, edited by W. S. Hoar and D. J. Randall. New York, Academic Press, pp. 253–292.
- Randall, D. J. and C. Daxboeck (1984). Oxygen and Carbon dioxide transfer across fish gills. In: *Fish Physiology*. Vol. XA, edited by W. S. Hoar and D. J. Randall. New York, Academic Press, pp. 263–314.
- Riley, R. L. and A. Cournand (1949). 'Ideal' alveolar air and the analysis of ventilation–perfusion relationships in the lungs. *J. Appl. Physiol.* 1: 825–847.
- Scheid, P. and J. Piiper (1971). Theoretical analysis of respiratory gas equilibration in water passing through fish gills. *Respir. Physiol.* 13: 305–318.
- Scheid, P. and J. Piiper (1976). Quantitative functional analysis of branchial gas transfer: Theory and application to *Scyliorhinus stellaris* (Elasmobranchii). In: *Respiration of Amphibious Vertebrates*, edited by G. M. Hughes. London – New York, Academic Press, pp. 17–38.
- Severinghaus J. W. (1971). Carbon dioxide solubility and first dissociation constant ( $pK'$ ) of carbonic acid in plasma and cerebrospinal fluid. In: *Handbook of Respiration and Circulation*, edited by P. L. Altman and D. S. Dittmer. Bethesda, Fed. Am. Soc. Exp. Biol., pp. 218–219.
- Siggaard-Andersen, O. (1974). *The Acid–Base Status of the Blood*. Copenhagen, Munksgård.
- Soivio, A. and H. Tuurala (1981). Structural and circulatory responses to hypoxia in the secondary lamellae of *Salmo gairdneri* gills at two temperatures. *J. Comp. Physiol.* 145: 37–43.
- Tuurala, H., P. Pärt, M. Nikinmaa and A. Soivio (1984). The basal channels of secondary lamellae in *Salmo gairdneri* gills – a non-respiratory shunt. *Comp. Biochem. Physiol.* 79: 35–39.
- Vogel, W. (1978). Arterio-venous anastomoses in the afferent region of trout gill filaments (*Salmo gairdneri*, Richardson). *Zoomorphologie* 90: 205–212.
- West, J. B. (1969). Ventilation–perfusion inequality and overall gas exchange in computer models of the lung. *Respir. Physiol.* 7: 88–110.
- Wood, C. M., B. R. McMahon and D. G. McDonald (1978). Oxygen exchange and vascular resistance in the totally perfused rainbow trout. *Am. J. Physiol.* 234: R201–R208.